COBEM 2023 27TH INTERNATIONAL CONGRESS OF MECHANICAL ENGENEERING

ABCM Brazilian Society of Mechanical Sciences and Engineering
27th ABCM International Congress of Mechanical Engineering
December 04-08, 2023, Florianópolis-SC, Brazil

COB-2023-1464
ANALYTICAL AND NUMERICAL DETERMINATION OF ACOUSTIC MODES OF 25 kN LIQUID PROPELLANT ROCKET ENGINE

Maurício Sá Gontijo
Mateus Silva Sant'Ana
Priscila Yukie Yamada
Aeronautics Institute of Technology
mauricio.sa.gontijo@gmail.com, mateussantana@ita.br, priscilayamada@ita.br

Renato de Brito do Nascimento Filho
Anieli Juliana Schrammel
DeltaV Engenharia Espacial
renato.nascimento@deltavengenharia.com, anieli.schrammel@deltavengenharia.com

Olexiy Shynkarenko
Jungpyo Lee
Artur Elias de Morais Bertoldi
University of Brasília
olexiy@aerospace.unb.br, jpleerocket@gmail.com, bertoldi@unb.br

Abstract. *Liquid propellant rocket engines are complex devices that work under extreme conditions and a wide range of pressure and temperatures. During operation, this type of engine is subject to several types of combustion instabilities, divided in low, intermediate and high frequency instabilities (in general, defined as 10 to 400 Hz, 400 to 1000 Hz and greater than 1000 Hz, respectively). These kinds of oscillations may cause chamber pressure peaks, which are a threat to the engine's performance and the thrust chamber and/or the vehicle's structural integrity. Thus, great efforts were conducted over the years to predict and suppress those phenomena. High frequency instabilities are commonly suppressed with baffles and acoustic cavities. In order to determine the necessity of those devices, acoustic analyses on the chamber are performed, since acoustic resonance might occur. In this work, a complete process of theoretical acoustic characterization was made on the new 25 kN Liquid Oxygen/Ethanol. This engine is being designed to be used on the new training rocket for launch centers, supported by the Brazilian government through the MCTI (Ministry of Science, Technology and Innovation), AEB (Brazilian Space Agency), FINEP (Financier of Studies and Projects) and FNDCT (National Fund for Scientific and Technological Development), and executed by DeltaV Engenharia Espacial. In this characterization, analytical calculations were validated with numerical simulations, with Finite Element Method (FEM). Those results will be used to, if necessary, design baffles or resonators. The eigenfrequencies were obtained analytically trough the based on the Helmholtz equation for a cylindrical combustion chamber closed at both sides (injector and throat), obtaining the roots of the Bessel function first derivative. In future works, the model will be validated with experimental tests and, finally, the obtained data will be used to design the rocket's structure and the test bench, to avoid its natural frequencies. The used methodology provides frequencies of the longitudinal, tangential and radial acoustic modes, both in hot and cold conditions. Cold condition is also of great interest, since it can contribute with relevant data and with fast and simple tests.*

Keywords: *Liquid Propellant Rocket Engines, Acoustics Modes, Numerical analysis*

1. INTRODUCTION

Liquid rocket engines are complex systems that operate under extreme conditions, involving the controlled combustion of propellants to generate high-pressure and high-temperature gases. The resulting combustion, turbulence and pressure fluctuations within these engines can give rise to acoustic waves and vibrations, which represent risk in engine performance and structural integrity. Also, the acoustic behavior can adversely affect engine efficiency, leading to decreased thrust or combustion instability.

Combustion instability occur from the intrinsic interaction between the combustion process and the acoustic modes present in the system. This instability occurs when the combustion process amplifies acoustic waves, which subsequently exerts an influence on the combustion process itself. The coupling between acoustic modes and combustion instability may induce self-sustained oscillations, significantly impacting on the engine's performance. Combustion instabilities

can be divided into low frequency (10 - 400 Hz), medium frequency (400 - 1000 Hz) and high frequency (> 1000 Hz) instabilities (Sutton and Biblarz, 1995).

The Liquid Propellant Rocket Engine (LPRE) to be studied in this work, DV-L25, is being developed by DeltaV Engenharia Espacial with the objective to be the main innovation on Brazilian training rockets, since until now only solid training rockets are used by Alcantara Launch Center and Barreira do Inferno Launch Center (CLA and CLBI, respectively - acronyms in Portuguese). This rocket engine aims to generate around of 25 kN of thrust for 10 s. It is a pressure-fed system with ablative thermal protection. Using Liquid Oxygen (LOx) and Ethanol as propellants, it is aligned with the Brazilian liquid propulsion program and it provides several new training capabilities, while being safe and green.

Several studies were performed previously to determine the acoustic modes of LPREs. These studies contains analytical, numerical and experimental analysis (Laudien *et al.*, 1995) (Souto *et al.*, 2007) (Santana Jr. *et al.*, 2007) (Pirk *et al.*, 2010) (Pereira *et al.*, 2013b) (Pereira *et al.*, 2013a) (Corá *et al.*, 2014) (Pirk *et al.*, 2015) (Guimarães *et al.*, 2015) (Araújo *et al.*, 2018) (Pirk *et al.*, 2021). However, there is a lack of publications that considers a chamber volume variation due to thermal protection consumption.

Thus, this paper proposes a study of determining acoustic frequencies and modes applied to the DV-L25 engine. This study aims to map the acoustic behavior of the engine analytically and numerically using the commercial software Ansys, for a hot and a cold case and checking the effects of a chamber volume variation. From the results obtained, it will be possible to plan future works from the experimental point of view.

2. METHODOLOGY

2.1 Analytical calculation

The acoustic modes are modeled mathematically, taking into account longitudinal, radial, tangential, and combined acoustic vibrations. For this, the parameters influencing the acoustic frequencies and mode are the geometry and the speed of sound of the gases inside the combustion chamber. To determine the speed of sound, both under hot and cold conditions, the following equation is used:

$$a = \sqrt{\gamma R T}, \tag{1}$$

where γ is the specific heat ratio, R is the gas constant ($R = R_u/M$, where R_u is the universal gas constant and M is the molecular weight of the gas) and T is the gas temperature.

In order to calculate the oscillation frequencies, the theory was developed considering a closed cylindrical chamber on both sides (injectors and nozzle) and by comparing with experimental results (Laudien *et al.*, 1995) (Natanzon, 1999). Shortening the mathematical path, the amplitude-phase frequency characteristic is defined in the form of a complex function as:

$$k\left(if\right) = \left|k\left(f\right)\right| e^{i\varphi(f)}, \tag{2}$$

where f is the oscillation frequency and φ is the phase of oscillations, which is calculated as:

$$\varphi_{m,n} = J_m\left(\frac{\beta_{m,n}R}{R_c}\right)\cos m\theta\left(\bar{X}^{+}_{m,n}e^{ik^{+}_{m,n}x} + \bar{X}^{-}_{m,n}e^{ik^{-}_{m,n}x}\right)e^{(ift)}, \tag{3}$$

where m and n are the tangential and radial mode numbers, J_m is the Bessel function, $\beta_{m,n}$ is the root of the Bessel function derivative,R is a radius, R_c is the chamber radius, $\bar{X}^{+}_{m,n}$ and $\bar{X}^{-}_{m,n}$ are arbitrary constants, θ is an angular coordinate and $k^{+}_{m,n}$ and $k^{-}_{m,n}$ are roots of the characteristic equation for determining the wave number $k_{m,n}$ defined as:

$$0 = -1\left(1 - M^2\right)k^2_{m,n} + 2MK_{m,n}\left(\frac{f}{a}\right) + \left(\frac{f}{a}\right)^2\alpha^2_{m,n}, \tag{4}$$

where M is the Mach number and $\alpha_{m,n}$ is defined below along with $k^{+}_{m,n}$ and $k^{-}_{m,n}$:

$$\alpha^2_{m,n} = 1 - \left(\frac{\beta_{m,n}a}{fR_c}\right)^2, \tag{5}$$

$$k^{+}_{m,n} = -\left(\frac{1}{1+M} + k^0_{m,n}\right)\frac{f}{a} \qquad ; \qquad k^{-}_{m,n} = \left(\frac{1}{1-M} + k^0_{m,n}\right)\frac{f}{a}, \tag{6}$$

where

$$k^0_{m,n} = \frac{-1 + \sqrt{M^2 - (1-M)^2 \alpha^2_{m,n}}}{1 - M^2}. \tag{7}$$

Stating, again, that both sides are closed and that at the injector $x = 0$, at the end $x = L$ (L is the length of the acoustic cavity) and that $M = 0$ (cylindrical cavity condition with impenetrable walls), therefore $\left.\frac{\partial \varphi_{m,n}}{\partial x}\right|_{x=0} = \left.\frac{\partial \varphi_{m,n}}{\partial x}\right|_{x=L} = 0$, Eq. (6) equals to:

$$k^+_{m,n} = -k^-_{m,n} = -\sqrt{\left(\frac{f}{a}\right)^2 - \left(\frac{\beta_{m,n}}{R_c}\right)^2}, \tag{8}$$

Applying Equation (8) on Equation (3) and using the closed cavity condition with impenetrable walls, the following relations are obtained:

$$-\bar{X}^+_{m,n} + \bar{X}^-_{m,n} = 0 \qquad ; \qquad -\bar{X}^+_{m,n} e^{ik^+_{m,n}L} + \bar{X}^-_{m,n} e^{-ik^-_{m,n}L} = 0. \tag{9}$$

Since the determinant of coefficients should vanish on the above system of equations (Natanzon, 1999), it is stated that $\sin x_{m,n}L =\therefore k^+_{m,n} = -\frac{\pi l}{L}$, where l is the longitudinal eigenvalues. Therefore, the following equation is used to calculate the natural frequencies of oscillation:

$$f = f_{m,n,l} = \frac{a}{2\pi}\sqrt{\frac{{\beta_{m,n}}^2}{{R_c}^2} + \frac{l^2\pi^2}{{L_e}^2}}, \tag{10}$$

where $\beta_{m,n}$ is the roots of the Bessel function derivative, R_c is the chamber radius and $L_e = L$, where L_e is the effective chamber length. The effective chamber length is defined as the chamber length plus one half of the nozzle convergent section length, in other words:

$$L_e = L_c + \frac{L_n}{2}. \tag{11}$$

The Bessel function is used for solving wave problems such as the propagation of sound waves and electromagnetic waves, as well as diffraction problems. The Bessel function can be divided into two main categories: Bessel functions of the first kind and Bessel functions of the second kind. Bessel functions of the first kind, denoted as J_m(x), are solutions of a second-order differential equation that arises in cylindrical or spherical wave problems. They describe the behavior of waves propagating radially from a central source. Bessel functions of the second kind, denoted as Y_m(x), are also solutions of a differential equation, but they become infinite or complex when x approaches zero. They describe the behavior of decreasing or diverging waves.

The Bessel functions are a family of mathematical functions that are solutions to Bessel's differential (Chakrabarti, 2006). The Bessel differential equation of order n is given by:

$$x^2\frac{d^2y}{dx^2} + x\frac{dy}{dx} + (x^2 - m^2)y = 0, \tag{12}$$

where y is the Bessel function of order m and x is the independent variable.

The general solution of this differential equation can be expressed as linear combination of the Bessel functions of the first kind (J_m(x)) and the second kind (Y_m (x)), along with multiplicative functions. The general form of the solution is:

$$y(x) = c_1 J_m(x) + c_2 Y_m(x), \tag{13}$$

where c_1 and c_2 are arbitrary constants.

The Bessel functions of the first kind (J_m(x)) are defined as:

$$J_m(x) = \frac{1}{\pi}\int_0^{\pi} \cos(m\theta - x\sin\theta)d\theta, \tag{14}$$

where θ is an angle, and the integral is known as the Bessel integral.

The Bessel functions of the second kind ($Y_m(x)$) are defined in a slightly more complex manner and are usually expressed in terms of the Bessel functions of the first kind. The roots of Bessel function, $\beta_{m,n}$ is also called as transversal eigenvalues and is easily obtained and some of its values are shown in Tab. 1.

Table 1: Some values of $\beta_{m,n} \therefore J'_m(x) = 0$.

n \ m	0	1	2	3	4	5
0	0	1.8412	3.0542	4.2012	5.3176	6.4156
1	3.8317	5.3314	6.7061	8.0152	9.2824	10.5199
2	7.0156	8.5363	9.9695	11.3459	12.6819	13.9872
3	10.1730	11.7060	13.1704	14.5859	15.9641	17.3128
4	13.3237	14.8636	16.3475	17.7887	19.1960	20.5755

The behavior of $\beta_{m,n}$ may also be analyzed graphically in Fig. 1.

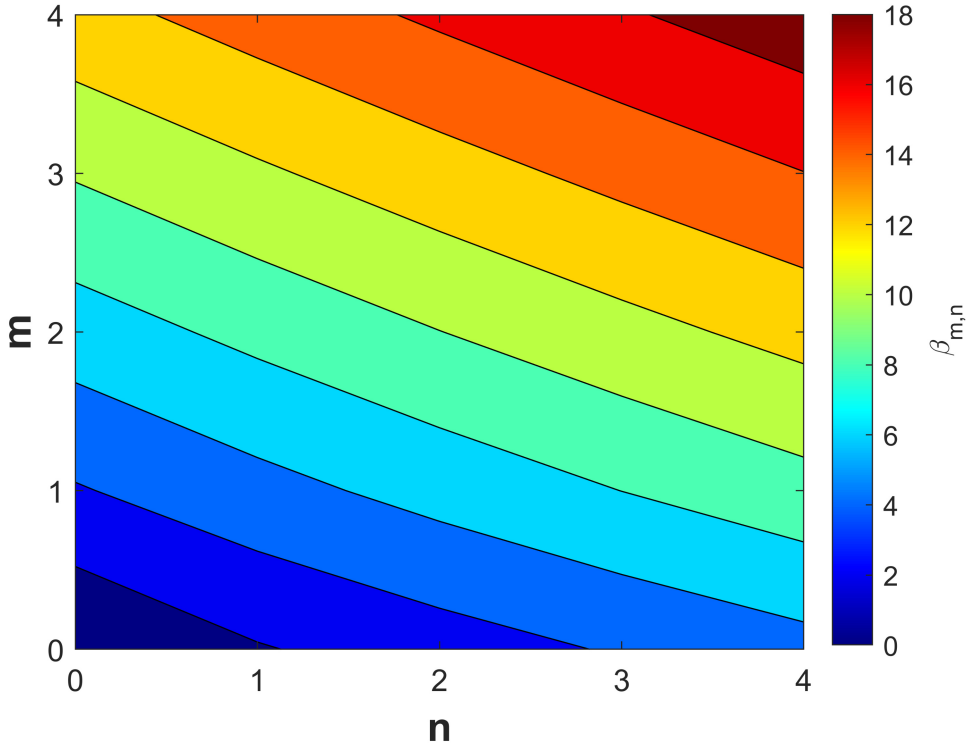

Figure 1: Behavior of β in function of m and n.

Under design possibilities, the main parameters that directly impacts the oscillation frequencies and that the designer has more control are the gas temperature, chamber radius and the effective length. As shown in Equation (1), the gas temperature inside the chamber impacts directly the sound speed, consequently affecting the frequency. In order to understand better the behavior of $f_{m,n,l}$ in function of T, the effective length was fixed in 493.40 mm, the chamber radius in 105.78 mm, the gas constant in 354.35 J/kgK and the specific heat ratio in 1.12, then T was varied. In addition, another analysis was made for different values of γ.

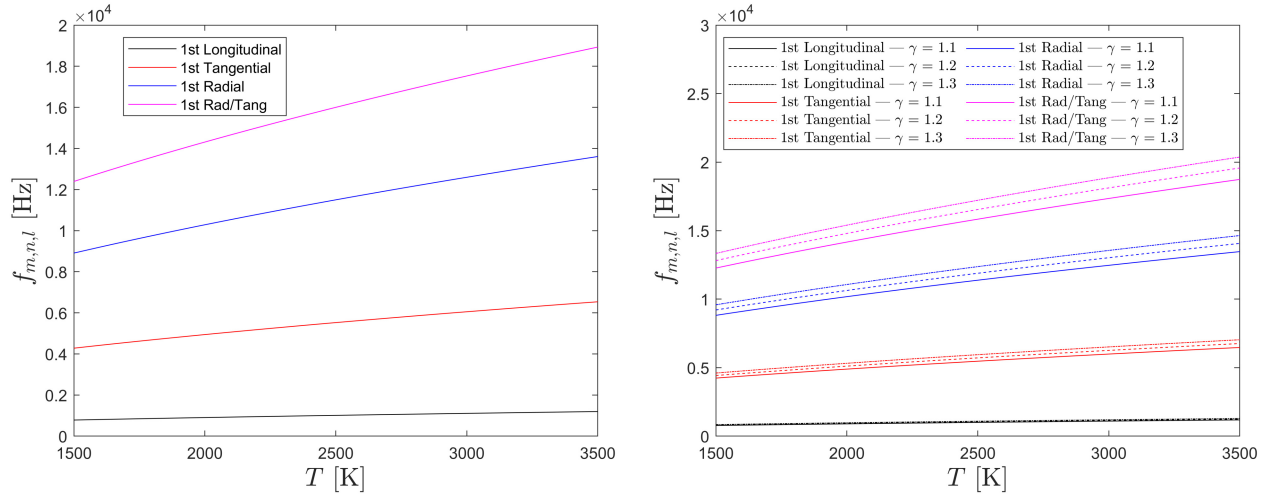

(a) (b)

Figure 2: (a) Behavior of $f_{m,n,l}$ in function of T, (b) Behavior of $f_{m,n,l}$ in function of T and γ.

As expected, the frequency is directly proportional to the gas temperature. Although, in Fig. 2b, it looks like for the 1st tangential mode there is no difference by varying the specific heat ratio value, it is just a matter of graph scale. However, the difference of $f_{m,n,l}$ between the three curves for this acoustic mode is significantly smaller than for the other modes, as is evidenced by the figure above. The other parameter that is easily controlled by the designer is the effective length. Now, fixing the sound speed in 1137.9 m/s and varying L_e and varying the chamber radius, the following graphs could be obtained:

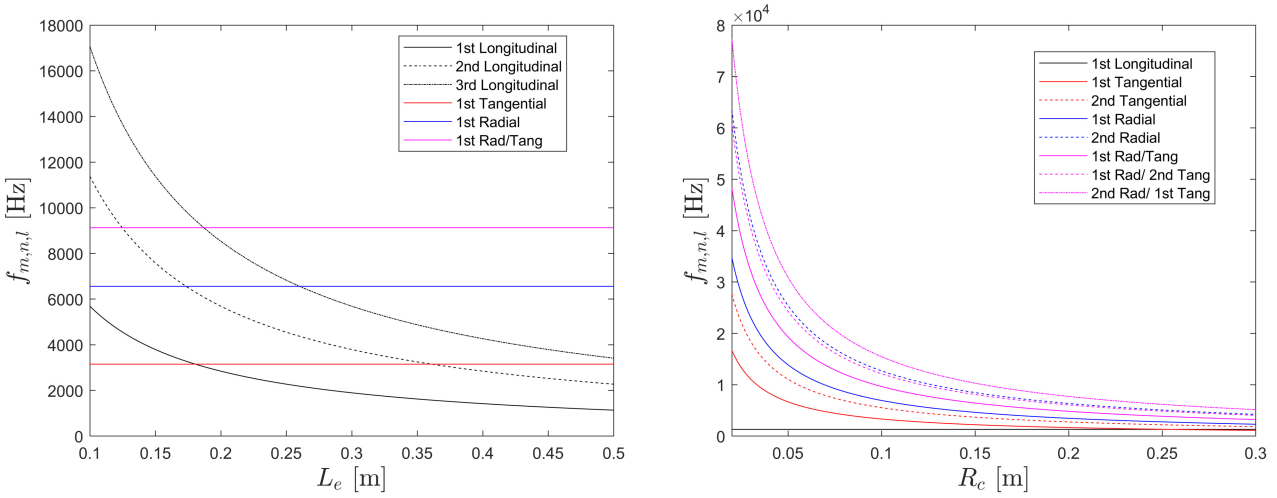

(a) (b)

Figure 3: (a) Behavior of $f_{m,n,l}$ in function of L_e, (b) Behavior of $f_{m,n,l}$ in function of R_c.

Thus, by analyzing Eq. (10) and Fig. 5a, the effective length only impacts the longitudinal acoustic modes. Analogously to the Fig. 5a and by easy comprehension of Equation (10), the chamber radius has no impact on the longitudinal modes. However, it highly affects radial and tangential modes.

The engine described above is shown in Fig. 4. The acoustic study is performed for the LPRE parameters in question in order to perform future studies and combustion instability analysis on the proposed design. In addition, the study provides acoustic combustion of the combustion chamber under hot gas and cold gas conditions.

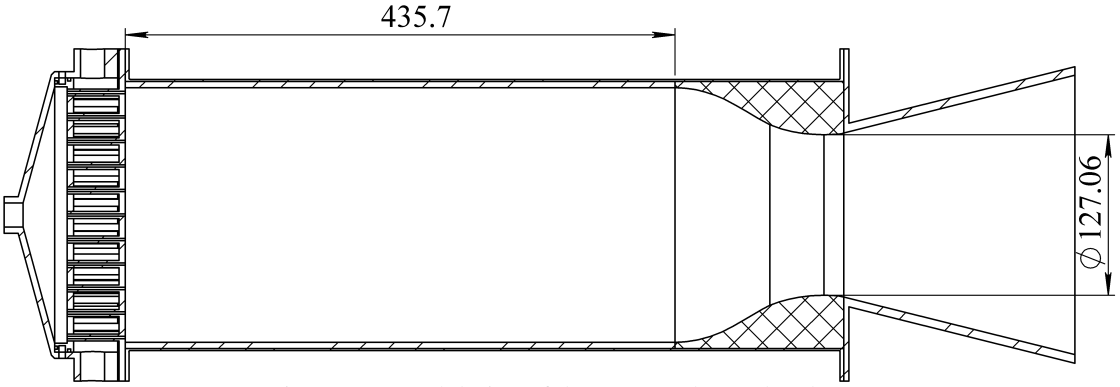

Figure 4: Actual design of the LPRE's thrust chamber

To determine the acoustic modes through the analytical approach, the sound speed in the combustion chamber was estimated considering hot and cold gas. In addition, since a ablative thermal protection is being used, the chamber radius varies during its operation, leading to a variation on $f_{m,n,l}$ ∴ Equation (10). The data used are compiled in Table 2.

Table 2: LPRE data

Cases	L_e**, mm**	R_c**, mm**	a**, m/s**
Hot & TP$^{(1)}$	493.40	100.78	1137.9
Cold & TP$^{(1)}$	493.40	100.78	343.11
Hot	493.40	105.78	1137.9
Cold	493.40	105.78	343.11

$^{(1)}$ TP = Thermal Protection.

The sound speed, and consequently γ, R and T, was obtained with Chemical Equilibrium with Applications (CEA) NASA's Software (Gordon and McBride, 1988) (McBride and Gordon, 1992) (McBride *et al.*, 1993) (McBride *et al.*, 1994) (Gordon and McBride, 1994) (Svehla, 1995) (McBride and Gordon, 1996) (McBride *et al.*, 2002).

2.2 Numerical calculation

The numerical formulation starts from the wave equation where it is considered homogeneous. Thus, the Helmholtz equation, Eq. (15), for acoustic cavity is used.

$$\nabla^2 p - \frac{1}{a^2}\frac{\partial^2 p}{\partial^2 t} = Q, \tag{15}$$

where p is the acoustic pressure, t is the time and Q is an acoustic source. From the equation described above, it is necessary to apply the boundary conditions (BC) in order to physically represent the case being analyzed. The BC can be defined in two categories, being a source condition or an impedance condition. Therefore, the source BC is defined according to Eq. (16).

$$\frac{\partial p}{\partial n} = -\rho\frac{\partial \nu_n}{\partial t}, \tag{16}$$

where n is the unit normal perpendicular to the surface, ρ is the density of the acoustic propagation medium, and $\nu_n$is the velocity normal to the surface. In addition to the source BC, the impedance BC is used. For this BC it is assumed that the boundary or wall is absorbing so that it is locally reactive. In this way the velocity normal to a surface depends only on the local pressure. Therefore, the impedance BC is defined according to Eq. (17).

$$\frac{\partial p}{\partial n} = -\frac{1}{a\zeta}\frac{\partial \nu_n}{\partial t}, \tag{17}$$

where ζ is a normalized impedance which depends on the specific acoustic impedance Z and is defined in Eq. 18.

$$\zeta = \frac{Z}{a\rho}. \tag{18}$$

For the parts of the acoustic domain frontier surrounded by rigid walls, that is, where the walls do not react to acoustic excitation the velocity of the acoustic particle is zero. Thus, for a rocket engine, the boundary conditions $\frac{\partial p}{\partial n} = 0$ must be applied. In this way, it is implied that $p = 0$. Rewriting the equation in its matrix form by applying the interpolation function N_f gives Eq. (19):

$$p = [N_f]\{p_n\}, \tag{19}$$

where $[\mathrm{N}_f]$ is the interpolation function and $\{\mathrm{p}_n\}$ is the nodal pressure vector. Discretizing the Helmholtz equation in case of acoustic fluid limited by rigid non absorbing walls, the kinetic and energy, Eq. (20), potential could be written.

$$T_f = \frac{1}{2}\{p_n\}^T[H]\{p_n\} \qquad ; \qquad U_f = \frac{1}{2\,e^2}\{\dot{p}_n\}^T[E]\{\dot{p}_n\}, \tag{20}$$

where $[E]$ and $[H]$ are the compressibility and volumetric matrices, respectively. Finally, the equation is discretized to apply the FEM with the rigid wall BC. Thus, the Lagrange formula for small oscillations is applied, resulting in Eq. (21).

$$[E]\{\ddot{p}_n\} + [H]\{p_n\} = \{0\}, \tag{21}$$

From the formulation presented it is possible to apply it to the internal volume of the LPRE under development. For the development of the numerical model the 3D geometry of the internal volume of the engine being the control volume corresponding to the combustion gases. To perform numerical calculation a geometry and mesh was created as show in Fig. 5a. In addition, it was checked whether the mesh developed meets the model. For this, the study of mesh convergence was performed in which the number of elements is varied in order to reach the mesh in which, for this case, the acoustic frequency is converged to some value, as shown in Fig. 5b.

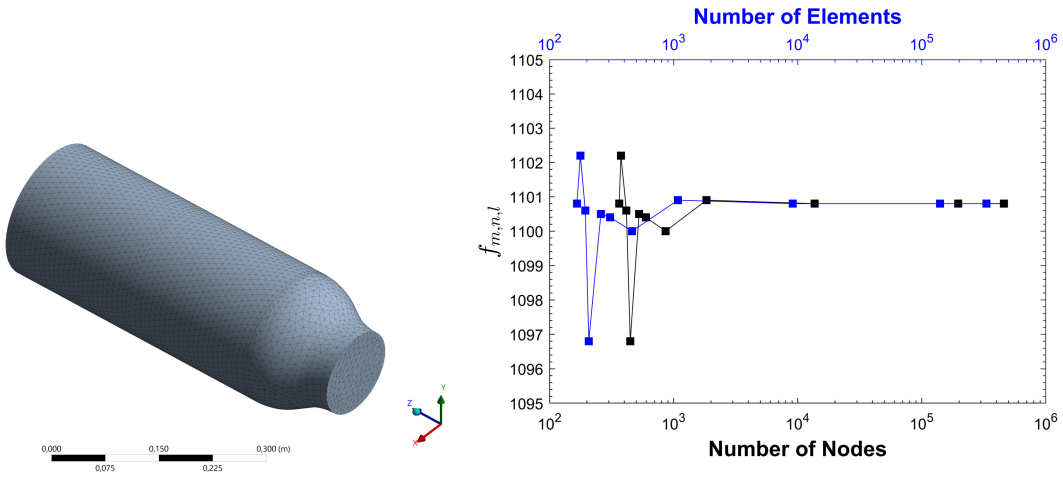

(a) (b)

Figure 5: (a) Geometry/Mesh, (b) Mesh convergence analysis.

Since no major difference was observed when comparing a structured and an unstructured mesh, for simplification an unstructured mesh was used. The control volume, according to Laudien *et al.* (1995) and Natanzon (1999), is from the injector face-plate until the nozzle throat. Studies have been carried out to check the influence of the divergent part of the nozzle, but results showed better agreement excluding this component Kekus (2022).

3. RESULTS

3.1 Analytical Results

Using Equation (10), theoretical analytical results were calculated and are compiled in Tab. 3. $f_{m,n,l}$ was calculated for 4 conditions: Hot & TP, Cold & TP, Hot and Cold; and values of R_c, L_e a for each condition are shown in Tab. 2. Furthermore, for each condition, 17 different acoustic modes were calculated, presented in the first column of Tab. 3. Each acoustic mode depends on a root of the Bessel function derivative, in this way, a linear combination between m, n, where $\beta_{m,n}$ is found in Tab. 1 or Fig. 1, is made. Also, the longitudinal eigenvalues are varied as $l = 1, 2, 3...$.

Table 3: Theoretical analytical results

Acoustic Mode	Orthogonal Directions			Hot & TP	Cold & TP	Hot	Cold
	m	n	l	Frequency, Hz			
1º Longitudinal	0	0	1	1153.12	347.70	1153.12	347.69
2º Longitudinal	0	0	2	2306.24	695.40	2306.24	695.40
3º Longitudinal	0	0	3	3459.36	1043.10	3459.36	1043.10
1º Tangential	1	0	0	3152.26	950.50	3152.25	997.65
2º Tangential	2	0	0	5228.99	1576.70	5228.99	1654.91
3º Tangential	3	0	0	7192.73	2168.82	7192.73	2276.42
1º Radial	0	1	0	6560.13	1978.07	6560.12	2076.21

3.2 Numerical Results

Some contours of the acoustic modes from the performed numerical simulations are presented in Fig. 6.

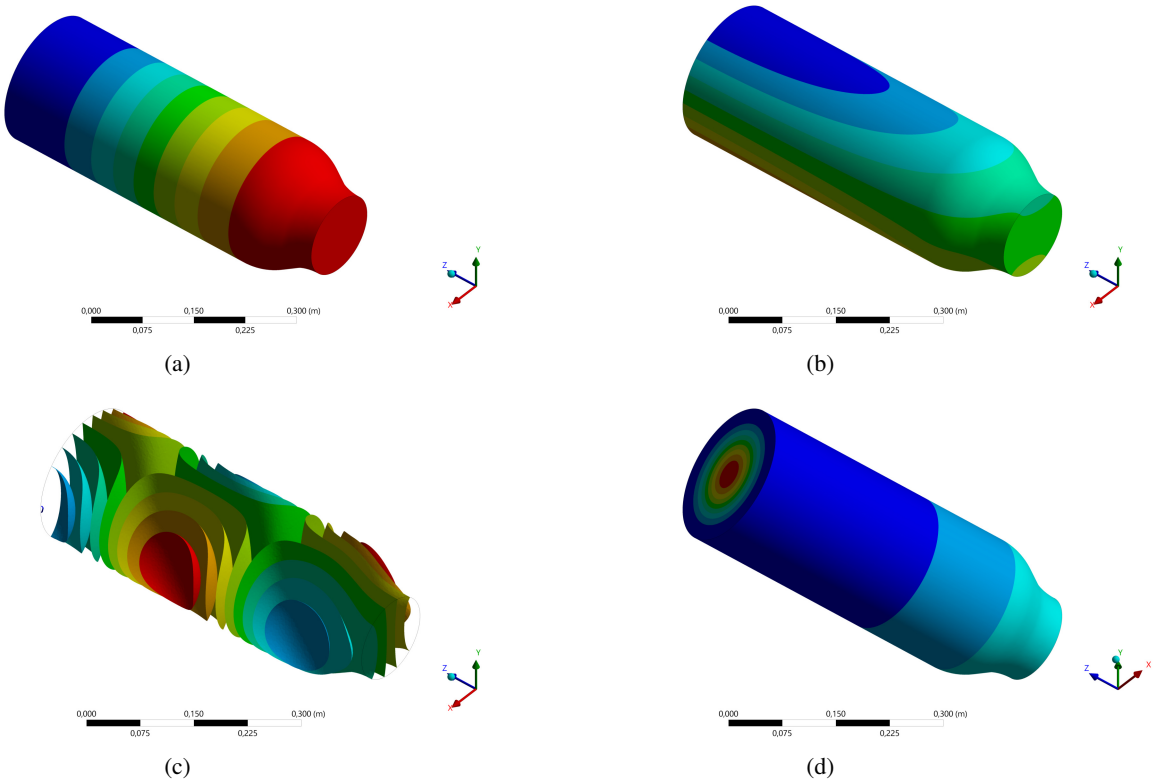

(a) (b) (c) (d)

Figure 6: (a) Longitudinal mode, (b) Tangential mode, (c) Longitudinal-Tangential mode (d) Radial mode.

On Figure 6d, the results were presented in iso-surface, while the other results in filled contours, for better visualization. In Table 4, it compiles all the results and comparisons between analytical and numerical calculations:

Table 4: Theoretical numerical results

Acoustic Mode	Hot & TP	Cold & TP	Hot	Cold	Error - Analytical Vs. Numerical, %			
	Frequency, Hz				Hot & TP	Cold & TP	Hot	Cold
1º Longitudinal	1100.80	331.93	1114.20	335.97	4.54	4.54	3.38	3.37
2º Longitudinal	2172.10	654.94	2183.30	658.33	5.82	5.82	5.33	5.33
3º Longitudinal	3179.10	958.58	3167.40	955.06	8.10	8.10	8.44	8.44
1º Tangential	3339.70	1007.00	3186.30	960.76	5.95	5.94	1.08	3.70
2º Tangential	5511.50	1661.90	5254.40	1584.40	5.40	5.40	0.49	4.26
3º Tangential	7567.90	2282.00	7213.00	2174.90	5.22	5.22	0.28	4.46
1º Radial	6907.80	2082.90	6584.30	1985.30	5.30	5.30	0.68	4.38

According to Laudien *et al.* (1995), the difference between the theoretical (hot) and experimental (cold) results is equal to the ratio of speeds of sound. This is easily observed when dividing Eq. (10) by itself, but under hot/cold conditions. This ratio, in this work, is equal to 3.316, from Tab. 2. Additionally, it is also possible to see that this statement is true by analyzing the results shown in Tabs. 3 and 4. Since previous works, conducted by Institute of Aeronautics and Space (IAE, in Portuguese) (Souto *et al.*, 2007) (Santana Jr. *et al.*, 2007) (Pirk *et al.*, 2010) (Pereira *et al.*, 2013b) (Pereira *et al.*, 2013a) (Corá *et al.*, 2014) (Pirk *et al.*, 2015) (Guimarães *et al.*, 2015) (Araújo *et al.*, 2018) (Pirk *et al.*, 2021), showed reasonable agreement between theoretical, numerical and experimental results, it is expected that the obtained results are reliable. However, in future, experimental tests will be conducted for validation.

4. CONCLUSIONS

This work presents an acoustic analysis of the new LPRE for a new Brazilian training rocket. Those analysis were divided in analytical and numerical simulations. Additionally, 4 conditions were simulated: Hot & TP, Cold & TP, Hot and Cold. Finally, the results were compared and presented to have reasonable agreements. The obtained data is quite relevant for a combustion chamber acoustic characterization, which is valuable information for designing this component and will be used on further developments.

The analytical and numerical correlation pointed out that for the cold condition of the gases is more sensitive to the variation of the radius of useful volume combustion chamber when compared to the hot case. The acoustic frequencies and the respective modes are coherent both compared to the theoretical and numerical values and to the literature. In addition, the ratio between the speeds of sound, under cold and hot conditions, was found to be 3.316.

In future, experimental tests will be conducted in order to characterize the combustion chamber and to compare with theoretical analysis, validating them. The experimental acoustic characterization supports the subsequent combustion instability studies during the product development and improvement process.

5. ACKNOWLEDGEMENTS

The authors would like to thank the MCTI (Ministry of Science, Technology and Innovation), AEB (Brazilian Space Agency), FINEP (Financier of Studies and Projects) and FNDCT (National Fund for Scientific and Technological Development) for funding (Grant term 03.22.0491.00 - FINEP reference project n° 1406/22 - Economic Subsidy for Innovation - n° 03/2022) the project and DeltaV Engenharia Espacial for the opportunity of developing such work.

6. REFERENCES

Araújo, T.B., Pirk, R., Souto, C.A., Almeida, D.S., Pagliuco, C.M.M., Nascimento, L.B., Pfuetzenreuter, L., Hardi, J.S., Preuss, A. and Langel, G., 2018. "Stability characteristics of the l75 lox-ethanol rocket engine". In *3AF Space Propulsion Confenrece*. 3AF - Association Aéronautique et Astrounautique de France.

Chakrabarti, A., 2006. *Elements Of Ordinary Differential Equations And Special Functions*. New Age International.

Corá, R., Martins, C.A. and Lacava, P.T., 2014. "Acoustic instabilities control using helmholtz resonators". *Applied Acoustics*, Vol. 77.

Gordon, S. and McBride, B.J., 1988. "Finite area combustor theoretical rocket performance". *NASA Technical Memorandum*, Vol. 100785.

Gordon, S. and McBride, B.J., 1994. "Computer program for calculation of complex chemical equilibrium compositions and applications - i analysis". *NASA Reference Publication*, Vol. 1311.

Guimarães, G.P., Pirk, R., Souto, C.A., Rett, S.R. and Góes, L.C.S., 2015. "Acoustic modes attenuation on rocket engines using helmholtz resonators: Experimental validation". In *15th International Conference on Experimental Mechanics*. EuraSEM - European Society for Experimental Mechanics.

Kekus, P., 2022. "Acoustic analysis of a liquid rocket engine: Approaches for tratment of nozzle flow". In *28th International Congress on Sound and Vibration*. IIAV - International Institute of Acoustics and Vibration.

Laudien, E., Pongratz, R., Pierro, R. and Preclik, D., 1995. *Experimental Procedures Aiding the Design of Acoustic Cavities*. Liquid Rocket Engine Combustion Instability, Progress in Astronautics and Aeronautics, Vol. 169, AIAA - American Institute of Aeronautics and Astronautics, Washington.

McBride, B.J. and Gordon, S., 1992. "Computer program for calculating and fitting thermodynamic functions". *NASA Reference Publication*, Vol. 1271.

McBride, B.J. and Gordon, S., 1996. "Computer program for calculation of complex chemical equilibrium compositions and applications - ii users manual and program description". *NASA Reference Publication*, Vol. 1311.

McBride, B.J., Gordon, S. and Reno, M.A., 1993. "Coefficients for calculating thermodynamic and transport properties of individual species". *NASA Technical Memorandum*, Vol. 4513.

McBride, B.J., Reno, M.A. and Gordon, S., 1994. "Cet93 and cetpc: An interim updated version of the nasa lewis computer program for calculating complex chemical equilibria with applications". *NASA Technical Memorandum*,

Vol. 4557.

McBride, B.J., Zehe, M.J. and Gordon, S., 2002. "Nasa glenn coefficients for calculating thermodynamic properties of individual species". *NASA Technical Papers*, Vol. 211556.

Natanzon, M.S., 1999. *Combustion Instability*. Progress in Astronautics and Aeronautics, Vol. 222, AIAA - American Institute of Aeronautics and Astronautics, Virginia.

Pereira, G.C.G., Pereira, L.F.S.M., Souto, C.A., Pirk, R. and Lacava, P.T., 2013a. "Acoustic characterization of a liquid-propellant rocket combustion chamber by numerical and analytical models". In *22nd International Congress of Mechanical Engineering*. ABCM - Brazilian Society of Mechanical Sciences.

Pereira, L.F.S.M., Pereira, G.C.G., Corá, R., Lacava, P.T. and Venson, G.G., 2013b. "Experimental validation of acoustic mode attenuation in combustion chamber using helmholtz resonator". In *22nd International Congress of Mechanical Engineering*. ABCM - Brazilian Society of Mechanical Sciences.

Pirk, R., Souto, C.A., Almeida, D.S., Pagliuco, C.M.M., Araujo, T.B. and Langel, L.P.G., 2021. "Stability assessment of l75 lox-ethanol rocket engine". *Journal of the Brazilian Society of Mechanical Sciences and Engineering*, Vol. 43.

Pirk, R., Souto, C.A., Araújo, T.B. and Almeida, D.S., 2015. "Modeling the acoustic behavior of a liquid rocket combustion chamber at room and operational conditions". In *23rd ABCM International Congress of Mechanical Engineering*. ABCM - Brazilian Society of Mechanical Sciences.

Pirk, R., Souto, C.A., Silveira, D.D., Souza, C.M. and Góes, L.C.S., 2010. "Liquid rocket combustion chamber acoustic characterization". *Journal of Aerospace Technology and Management*, Vol. 2.

Santana Jr., A., Silva, M.S., Lacava, P.T. and Góes, L.C.S., 2007. "Acoustic cavities design procedures". *Thermal Engineering*, Vol. 6.

Souto, C.A., Souza, C.M. and Pirk, R., 2007. "Acoustic modes of a liquid propelled rocket combustion chamber". In *6º Brazilian Conference on Dynamics, Control and Their Applications - Dincon*. ABCM and SBMAC - Brazilian Society of Mechanical Sciences and Engineering Brazilian Society of Applied and Computational Mathematics, respectively, São José do Rio Preto, SP, Brazil.

Sutton, G.P. and Biblarz, O., 1995. *Rocket propulsion elements*. John Wiley Sons, 9th Ed., Hoboken.

Svehla, R.A., 1995. "Transport coefficients for the nasa lewis chemical equilibrium program". *NASA Technical Memorandum*, Vol. 4647.

7. RESPONSIBILITY NOTICE

The authors are solely responsible for the printed material included in this paper.